Mem. S.A.It. Suppl. Vol. 22, 164

Memorie della
Supplementi

The primordial helium abundance: no problem

E. Skillman[1,2], E. Aver[2,1], and K. Olive[2,1]

[1] Minnesota Institute for Astrophysics
[2] University of Minnesota, School of Physics and Astronomy
e-mail: skillman@astro.umn.edu

Abstract. We have used Markov Chain Monte Carlo (MCMC) techniques to analyze the large dataset of Izotov, Thuan, and Stasinska. We draw attention to the use of χ^2 as a clear measure of the quality of the physical solution for individual spectra and adopt this measure in order to cut the sample to reliable solutions. We also emphasize the importance of the He I λ4026 emission line for its sensitivity to underlying absorption. The final dataset, after cuts, exhibits improved consistency. Regression to zero metallicity yields Y_p = 0.2534 ± 0.0083, in agreement with the WMAP result of 0.2487 ± 0.0002. Using the same dataset, Izotov and Thuan have argued that their derived value of the primordial helium abundance (Y_p) is inconsistent with the value derived from WMAP assuming standard big bang nucleosynthesis, in the sense that their determination is too high by two sigma. Our result indicates that it is premature to emphasize a discrepancy.

Key words. big bang nucleosynthesis, primordial helium

1. Introduction

Next to the cosmic microwave background radiation, standard big bang nucleosynthesis (SBBN) is the most robust probe of the early universe available (Walker et al. 1991; Olive et al. 2000). Furthermore, using the precise baryon density as determined by WMAP (Komatsu et al. 2011), SBBN has effectively become a parameter free theory (Cyburt et al. 2002). As such, one can use SBBN to make relatively precise predictions of the initial light element abundances of D, ^{3}He, ^{4}He, and ^{7}Li (e.g., Coc et al. 2011, and references therein). Therefore, an observational determination of these abundances becomes a test of the concordance between SBBN theory and the analyses of microwave background anisotropies. To test these predictions, the observed abundances must be determined with relatively high precision. Unfortunately, there is a logarithmic relationship between the baryon to photon ratio, η, and the primordial helium abundance, Y_p. Thus, any meaningful test of the theory requires a determination of Y_p to an accuracy of $\lesssim$ 1%. The 7-year WMAP value for η is $(6.19 \pm 0.15) \times 10^{-10}$ (Komatsu et al. 2011). For comparison, the SBBN calculation of Cyburt et al. (2008), assuming the WMAP η and a neutron mean life of 885.7 ± 0.8 s (Nakamura et al. 2010), yields Y_p = 0.2487 ± 0.0002, a relative uncertainty of only 0.08%.

Here, we discuss the determination of Y_p using observations of low metallicity H II regions in dwarf galaxies. By fitting the helium abundance versus metallicity, one can extrapolate back to very low metallicity, corresponding to the primordial helium abundance

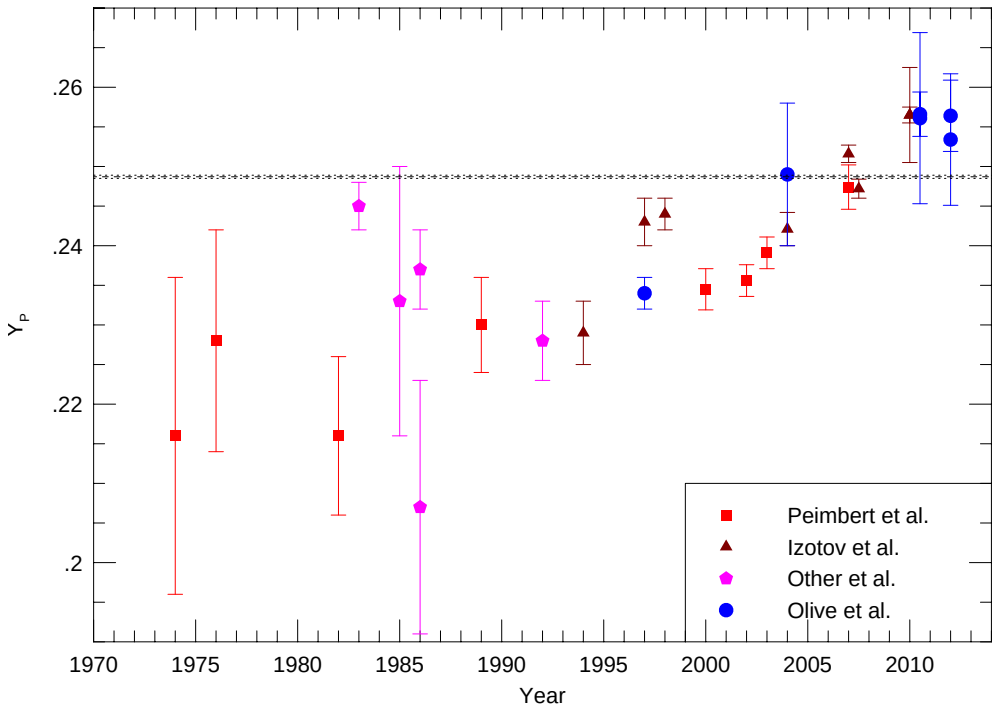

Fig. 1. A history of measurements of Y_p. For the Izotov et al. (2010) data point, the smaller error bars indicate the statistical error while the larger error bars include a systematic error estimate. For our work in 2010 and 2012, the smaller error bars are a result of averaging data points, while the larger error bars result from a regression to primodial abundance.

(Peimbert & Torres-Peimbert 1974). The oxygen to hydrogen ratio, O/H, commonly serves as a proxy for metallicity. The difficulties in calculating an accurate and precise measure of the primordial helium abundance are well established (Olive & Skillman 2001, 2004; Izotov et al. 2007).

Izotov & Thuan (2010) point to modern measurements of Y_p as indicative of evidence for non-standard big bang nucleosynthesis. They present a determination of Y_p based on 93 spectra of 86 low-metallicity extragalactic H II regions (the HeBCD sample, Izotov et al. 2007, ITS07) and taking into account recent developments concerning systematic effects. They find a value of $Y_p = 0.2565 \pm 0.0010$ (stat.) $\pm$ 0.0050 (syst.), and state that this value is higher at the 2σ level than the value given by standard big bang nucleosynthesis. They further point out that if this difference is attributed entirely to the effective number of light neutrino species, then N_ν is equal to $3.68^{+0.80}_{-0.70}$ (2σ) or $3.80^{+0.80}_{-0.70}$ (2σ) for a neutron lifetime (τ_n) equal to 885.4 $\pm$ 0.9 s or 878.5 $\pm$ 0.8 s, respectively, which is significantly larger than the expected value of 3.

Note, however, that the history of measurements of Y_p has had some blemishes (see figure 1). There appears to be consensus that the dominating uncertainties are systematic, and much of the recent effort has gone into understanding those systemic effects. Thus, using measurements of Y_p in order to promote departures from standard big bang nucleosynthesis can be approached with a measure of skepticism.

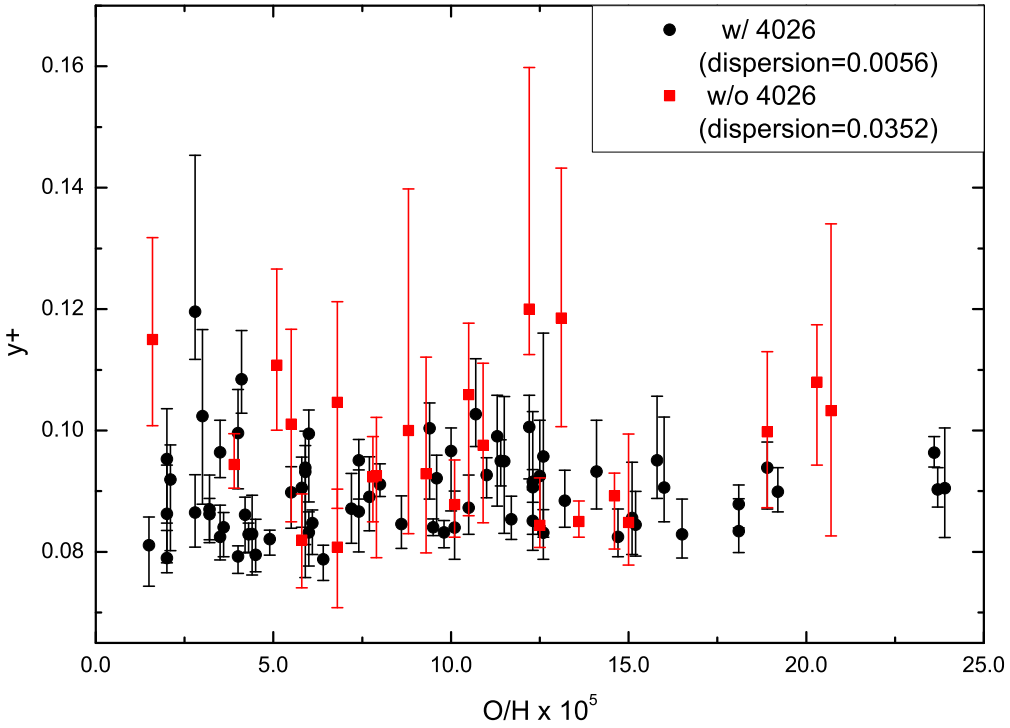

Fig. 2. Plot of the helium abundance versus O/H for the entire sample. The black circles denote objects for which He I λ4026 is reported and was used to calculate χ^2 and determine the best-fit solution, while the red squares mark objects for which He I λ4026 is not reported and is, therefore, excluded from their analysis. An upward bias in the value of y^+ is apparent in the distribution of points lacking He I λ4026. (from Aver et al. 2012)

In previous analyses, we have emphasized that because of the degeneracies in solutions for the physical conditions in the H II regions, it is absolutely essential to use Monte Carlo analyses in order to estimate the true uncertainties on individual observations (Olive & Skillman 2001, 2004; Aver et al. 2010). Specifically, in Aver et al. (2010), we explored (a) the effects of new He I emissivities, (b) "integrating" the H I and He I lines in a single minimization, (c) better treatments of underlying absorption, and (d) solving for HI collisional excitation. Since only a small number of high quality spectra were analyzed, this resulted in a relatively large uncertainty in the predicted value of Y_p.

Following that, we introduced a new method based on Markov Chain Monte Carlo (MCMC) techniques (Aver et al. 2011, AOS2). Our MCMC method is superior to previous implementations (free from biases due to non-physical parameter space). In addition, the MCMC analysis allows a detailed exploration of degeneracies, and, in particular, a false minimum at large values of optical depth in the He I emission lines. Also, introducing the [O III] temperature as a prior, in a very conservative manner, produces negligible bias and effectively eliminates the false minima occurring at large optical depth.

Recently, in Aver et al. (2012), we have systematically applied this technique to the data compiled in (Izotov et al. 2007, ITS07). Here I will report on the results of these efforts.

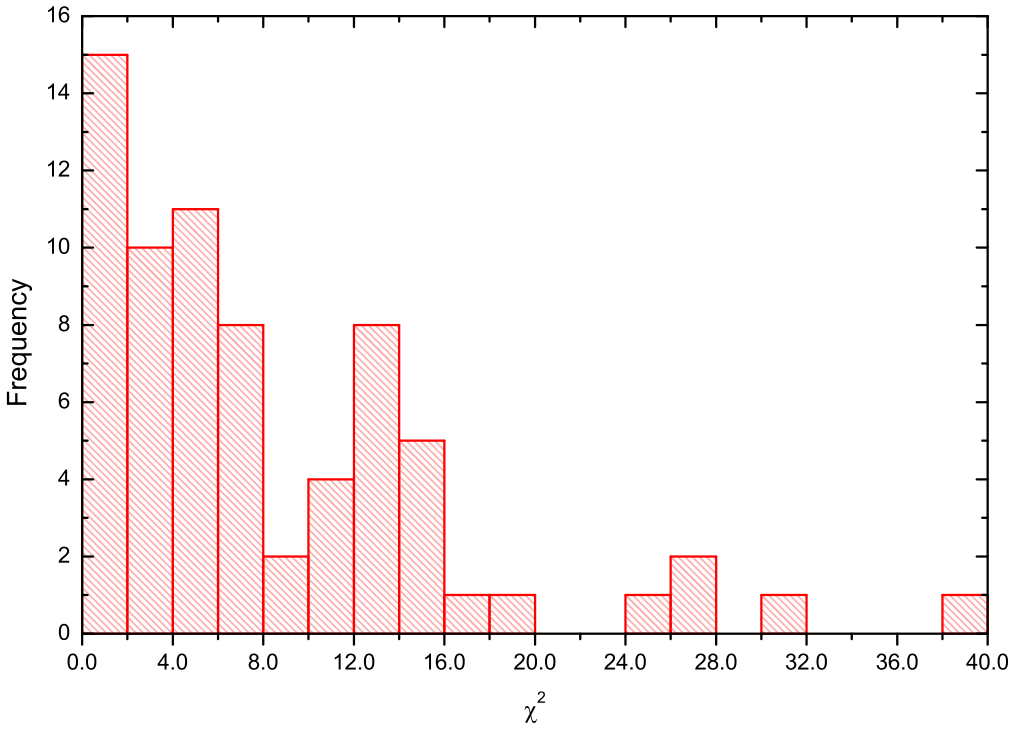

Fig. 3. Histogram of best-fit χ^2 for the 70 observations with He I λ4026 reported. 25 observations have $\chi^2 < 4$ (95.45% confidence level). (from Aver et al. 2012)

2. The importance of He I λ4026

For 23 of the 93 observations in the HeBCD sample, the weak line He I λ4026 is not detected. These objects can still be analyzed, with the helium χ^2 composed of the sum of the remaining five He lines. To help evaluate the reliability of these 23 objects, the impact of removing He I λ4026 is investigated in five H II regions. These galaxies were chosen to sample a range of equivalent widths: SBS 0917+527, HS 0924+3821, SBS 1152+579, Mrk 209, and SBS 0940+544 2, with W(Hβ) of 87, 114, 189, 224, and 241 Å, respectively. An eight parameter fit to yield the minimum χ^2 was performed and uncertainties were calculated from $\Delta\chi^2$. Note that without He I λ4026, the system is, in principle, no longer overdetermined; though due to degeneracies, a "perfect $\chi^2 = 0$" is not found.

the most significant effect of removing He I λ4026 is on the value of a_{He}, which increases by 0.23 Å, on average, which is larger than the typical uncertainty in the solutions including He I λ4026. The average fractional increase is 69%. The uncertainty on a_{He} also increases notably, with the average uncertainty tripling. None of the other determinations of physical conditions show a similar significant bias with the absence of a He I λ4026 measurement. Since the correction for underlying helium absorption translates linearly into the helium abundance, increases in the underlying helium absorption directly lead to an increase in y^+ for all five objects, with an average fractional increase of 4%. Clearly this is an unacceptable bias when the ultimate goal is an uncertainty on the order of $\sim$ 1%.

This systematic bias is demonstrated in figure 2, which shows the helium abundances for all 93 objects. The set of 23 observations with-

out He I λ4026 exhibits bias toward higher values of y^+, with a subset of these objects noticeably elevated from the majority of the points with He I λ4026. A calculation of the mean for each population underscores the shift; the mean abundance for the 70 objects with He I λ4026 is $< y^+ >= 0.0867 \pm 0.0056$, while it is $< y^+ >= 0.0900 \pm 0.0352$ for the 23 without He I λ4026. The uncertainties reported with each $< y^+ >$ are the dispersions of the sample. The seven-fold increase in dispersion for the sample without He I λ4026 demonstrates its unreliability.

3. Using chi-squared as an analysis tool

After dropping the 23 objects without λ4026 measurements, 70 objects remain. Figure 3 shows the distribution of χ^2 values for the solutions for these remaining 70 objects. Clearly, not all solutions provide good fits to the data (as evidenced by relatively high values of χ^2). Fits with large χ^2 may indicate a measurement discrepancy in the line fluxes, an underestimation of the uncertainties, or the possibility that the model used to derive abundances is inappropriate for the object under study. In any case, points with large χ^2 are not reliable, and thus, we exclude them from further analysis in determining Y_p. There are nine observed line ratios used to calculate χ^2 and eight model parameters fit to the data; thus, there is only one degree of freedom, modulo correlations. Here we choose to cut the sample at a standard value of $\chi^2 < 4$, corresponding to a 95.45% confidence level. This cut removes 45 observations, leaving 25 (figure 3). The disappointing result that nearly two-thirds of the sample have solutions with such low likelihoods ($\chi^2 > 4$) is troubling and warrants further investigation. At this point, we cannot be certain whether this result is due to deficiencies in the model, the observations and their errors, or both.

4. Results from the final dataset

The 22 objects for which the model is a good fit, which return physically meaningful parameter solutions, and which provide a robust metallicity baseline for regression comprise the Final Dataset, which we use to determine Y_p. Figure 4 presents the derived y^+ values as a function of O/H. Seven objects flagged for large outlier values of τ, a_H, a_He, and ξ are highlighted with different symbols in figure 4. These flagged data points show a possible systematic shift to larger values of y^+; the average value of y^+ for the flagged objects is 9% higher than that of the unflagged objects in the Final Dataset.

The primary goal of this work, the primordial helium abundance (mass fraction), Y_p, can now be calculated for several subsets of the final dataset. A regression of Y, the helium mass fraction, versus O/H, the oxygen to hydrogen mass fraction, is used to extrapolate to the primordial value[1]. The O/H values are taken directly from ITS07.

Because it minimizes confounding systematic effects, our preferred dataset is the 14 qualifying points. The regression yields,

$$Y_p = 0.2534 \pm 0.0083, \quad (1)$$

with a slope of 54 ± 102 and a χ^2 of 2.9. The result is shown in figure 5. Note that the expected value of χ^2 for this dataset is ~ 12, so the resultant χ^2 is unexpectedly low. This result for Y_p agrees well with the WMAP value of $Y_p = 0.2487 \pm 0.0002$. AOS2 determined $Y_p = 0.2609 \pm 0.0117$ ($0.2573^{+0.0033}_{-0.0088}$ with the slope restricted to be positive). Given their large uncertainties, these results are in agreement with the newer result. The smaller uncertainty on the unconstrained fit is a direct result of the increased sample size (doubling from 7 objects in AOS2 to 14 here).

Because the uncertainty in the slope of the He regression is large, it will be difficult to use this result to constrain models of chemical evolution. We do note however, that simple models of galactic chemical evolution tend to predict dY/dZ values of order 1, with higher values (of order 3) being possible when enriched winds are included (Pilyugin 1993; Fields & Olive 1998) (our result corresponds to roughly $dY/dZ = 2.7 \pm 5.1$). For comparison, studies of

[1] This work takes $Z = 20(O/H)$ such that $Y = \frac{4y(1-20(O/H))}{1+4y}$

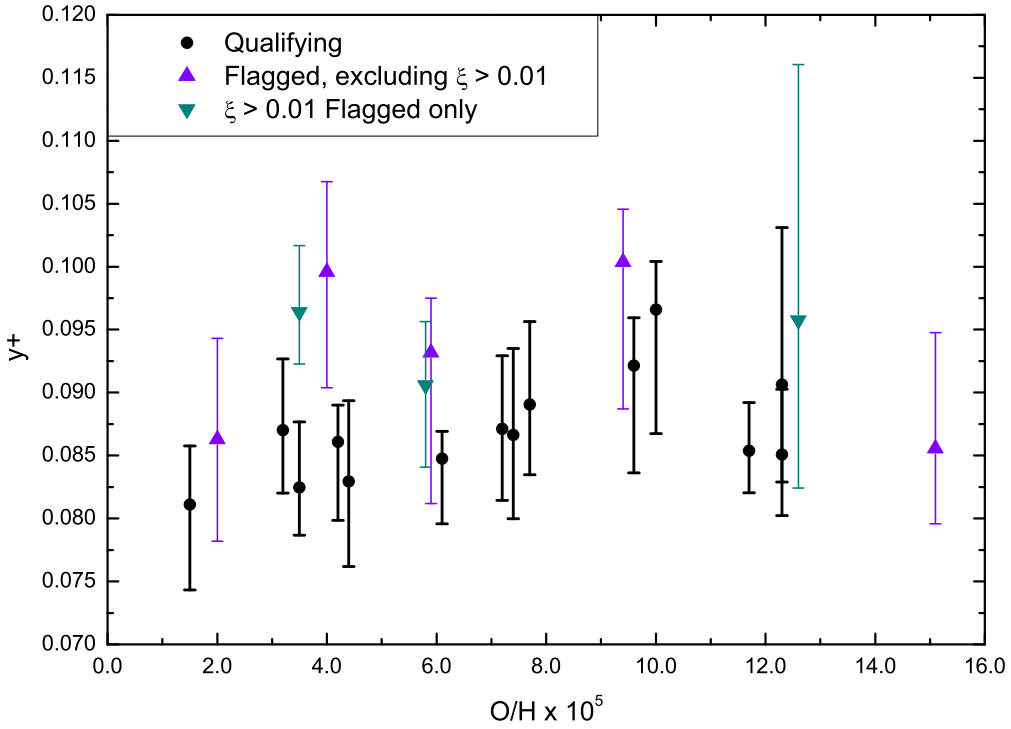

Fig. 4. Plot of y^+ vs O/H for the 22 objects meeting the prescribed reliability standards. The upward triangles signify points flagged for large outlier values in optical depth or underlying absorption. The downward triangles signify points flagged for large neutral hydrogen fractions. (from Aver et al. 2012)

Galactic dY/dZ also typically find between 1 and 3 Pagel & Portinari (1998); Casagrande et al. (2007); Balser (2006).

As the O/H domain is limited, an estimate of Y_p using the mean value is justified and gives,

$$Y_p = 0.2574 \pm 0.0036. \quad (2)$$

This is not significantly different from the result of the regression fit; however, the uncertainty is decreased by more than a factor of two.

Including the flagged objects raises the intercept and reduces error to 0.2611 ± 0.0067 with a slope of 0 ± 86. The reduced uncertainty is a result of the increased number of points in the regression, and the possible systematic bias toward larger y^+ within the flagged dataset raises the intercept. Olive & Skillman (2004) restricted the metallicity baseline to $O/H = 9.2 \times 10^{-5}$. Adopting the same metallicity cut with the dataset of this work decreases the intercept substantially to 0.2465 ± 0.0134 and produces a strongly positive slope (though still consistent with 0) of 196 ± 230. Using all 93 observations included in their HeBCD sample, ITS07 determined $Y_p = 0.2516 \pm 0.0011$. Their much smaller uncertainty is achieved primarily though the use of the full sample of observations. Inspection of figure 1 shows relatively good agreement between ITS07 and the present results, with small but significant differences in the size of the uncertainties. Following our analysis, there is no current discrepancy between the value of Y_p inferred from observations of metal-poor H II regions and that derived from CMB observations assuming standard big bang nucleosynthesis.

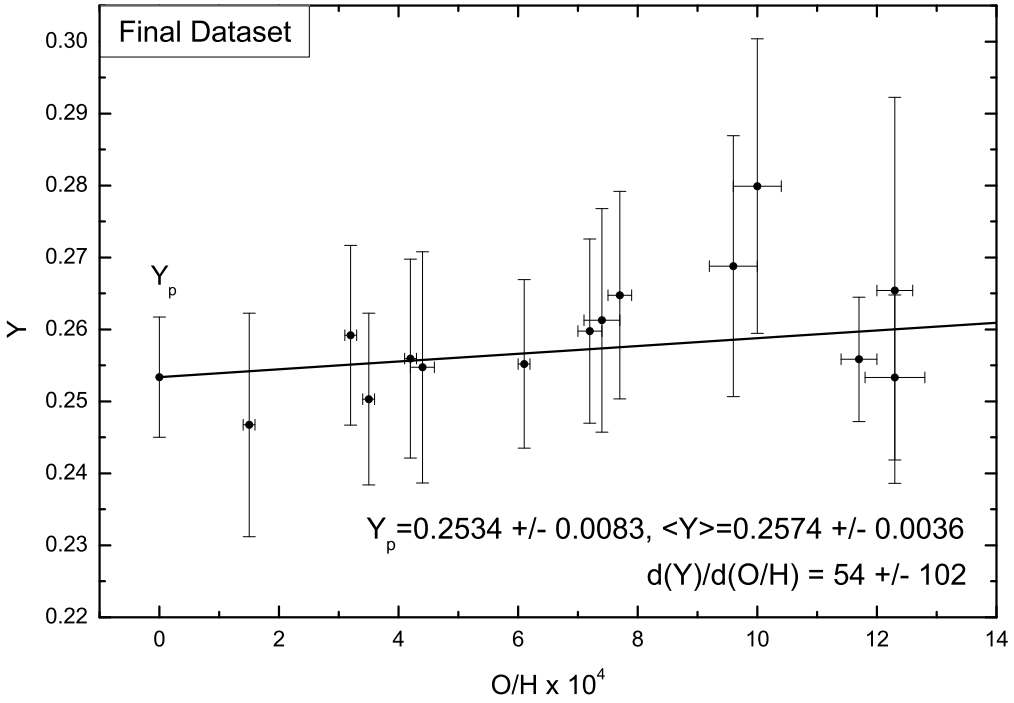

Fig. 5. Helium abundance (mass fraction) versus oxygen to hydrogen ratio regression calculating the primordial helium abundance. (from Aver et al. 2012)

5. Conclusions

In summary, we have demonstrated the rigor and transparency of MCMC methods in selecting the best available data to ultimately extract the primordial He abundance. It supports a stringent screening of candidate spectra, yielding a robust sample. The fruit of these labors is an improved determination of the primordial helium abundance, both in increased confidence in its accuracy and in a modest increase in its precision. These uncertainties are still relatively large, however, and the case for needing higher quality spectra is further strengthened.

Acknowledgements. We are very grateful to the SOC for the opportunity to present our recent findings and, especially, for organizing such an exciting, informative, and enjoyable conference. We wish to thank Yuri Izotov for encouraging us to expand our analysis to a larger dataset and for providing the λ4026 measurements for the HeBCD sample. The work of EA and KAO is supported in part by DOE grant DE-FG02-94ER-40823. EDS is grateful for partial support from the University of Minnesota. We are especially grateful to the referees of our papers who have been very helpful and supportive.

References

Aver, E., Olive, K. A., & Skillman, E. D. 2010, JCAP, 5, 3

Aver, E., Olive, K. A., & Skillman, E. D. 2011, JCAP, 3, 43

Aver, E., Olive, K. A., & Skillman, E. D. 2012, JCAP, 4, 4

Balser, D. S. 2006, AJ, 132, 2326

Casagrande, L., Flynn, C., Portinari, L., Girardi, L., & Jimenez, R. 2007, MNRAS, 382, 1516

Coc, A., Goriely, S., Xu, Y., Saimpert, M., & Vangioni, E. 2011, arXiv:1107.1117

Cyburt, R. H., Fields, B. D., & Olive, K. A. 2002, Astroparticle Physics, 17, 87

Cyburt, R. H., Fields, B. D., & Olive, K. A. 2008, JCAP, 11, 12

Fields, B. D., & Olive, K. A. 1998, ApJ, 506, 177
Izotov, Y. I., Thuan, T. X., & Stasińska, G. 2007, ApJ, 662, 15
Izotov, Y. I., & Thuan, T. X. 2010, ApJ, 710, L67
Komatsu, E., Smith, K. M., Dunkley, J., et al. 2011, ApJS, 192, 18
Nakamura, K. et al. [Particle Data Group] 2010 J. Phys. G, 37, 075021
Olive, K. A., & Skillman, E. D. 2001, New Astron., 6, 119
Olive, K. A., & Skillman, E. D. 2004, ApJ, 617, 29
Olive, K. A., Steigman, G., & Walker, T. P. 2000, Phys. Rep., 333, 389
Pagel, B. E. J., & Portinari, L. 1998, MNRAS, 298, 747
Peimbert, M., & Torres-Peimbert, S. 1974, ApJ, 193, 327
Pilyugin, L. S. 1993, A&A, 277, 42
Walker, T. P., Steigman, G., Kang, H.-S., Schramm, D. M., & Olive, K. A. 1991, ApJ, 376, 51